NMRlipids IV: Headgroup & glycerol backbone structures, and cation binding in bilayers with PS lipids

O. H. Samuli Ollila[1,2,*] and NMRlipids collaboration 1.Authorship query to be sent soon.[3]

[1]*Institute of Organic Chemistry and Biochemistry, Academy of Sciences of the Czech Republic, Prague 6, Czech Republic*
[2]*Institute of Biotechnology, University of Helsinki*
[3]*nmrlipids.blogspot.fi*

(Dated: May 23, 2018)

Primarily measured but also simulated NMR order parameters will be collected also for other than phophatidylcholine (these are discussed in NMRlipids I) headgroup. The information will be used to understand structural differences between different lipid molecules in bilayers.

INTRODUCTION

Phosphatidylserine (PS) is the most common negatively charged lipid in eykaryotic membranes. PS lipids compose 8.5% of total lipid weight of erythrocytes, but the abundance varies between different organelles up to 25-35% in plasma membrane [1–3]. Despite of the relatively low abundance, PS lipids are important signaling molecules. They interact with signaling proteins [2], regulate surface charge and protein localization [4], and induce protein aggregation [5, 6]. Some domains spesifically interact PS lipids, while others are attracted by general electrostatics and the binding can be regulated by calcium [2]. Therefore, the structural details of lipid headgroups and the details of calcium binding are crucial for the PS mediated signaling processes.

The structure of PS lipid headgroups and their interactions with ions have been studied with various experimental methods and theoretical techniques [7**?** , 8]. However, the consesus has not been reached due to the difficulties to interpret the experimental data [**?**] and the inaccuracies in simulation models at the headgroup region [9–11]. Some studies propose that the negatively charged lipids attract cations only due to the increase of local concentration in the vicinity of membranes and that the binding constant of cations is similar to zwitterionic and negatively charged lipids [12**?** , 13]. On the other hand, some studies propose specific binding of calcium directly to PS lipid headgroups [14**?** , 15], The NMR data proposes that the PS headgroup is more rigid than PC,PE or PG headgroups, but more detailed interperetation has not been done.

Headgroup and glycerol backbone C-H bond order parameters calculated from MD simulations have been recently used to interpret the lipid structures in NMR experiments and to validate lipid structure and ion binding in simulations of PC lipid bilayers [9–11, 16]. In this work we apply this approach to PS lipid headgroup in order to elucidate the structural details and ion binding to negatively charged lipids. The results are expected to elucidate also PS mediated signalling events because glycerol backbone and headgroup structure and behaviour are similar in model membranes and in bacteria [12, 17, 18].

METHODS

Solid state NMR experiments

The magnitude and signs of the C-H bond order parameters in headgroup and glycerol backbone were measured using natural abundance ^{13}C solid state NMR spectroscopy as described previously [16, 19]. Shortly, the absolute values of the order parameters were determined from the dipolar splittings given by the indirect dimension of 2D R-PDFL experiment [20] and the signs were measured using S-DROSS experiments [21].

2.Details of the used spectrometer and maybe some other details should be given.

3.Sample preparation should be described.

Molecular dynamics simulations

Molecular dynamics simulation data was collected using the Open Collaboration method [9]. The NMRlipids project blog (`nmrlipids.blogspot.fi`) and the GitHub repository (`github.com/NMRLipids/NMRlipidsIVotherHGs`) were used as the communication platforms. The simulated systems are listed in Table II and simulation details are given in the SI. The simulation data is also indexed in the searchable database (`nmrlipids.fi`), and in the NMRlipids/MATCH GitHub repository (`https://github.com/NMRLipids/MATCH`).

The C-H bond order parameters were calculated directly from the definition

$$S_{\mathrm{CH}} = \frac{1}{2}\langle 3\cos^2\theta - 1\rangle, \qquad (1)$$

where θ is the angle between the C-H bond and the membrane normal. Angular brackets point to the average over all sampled configurations.

TABLE I: List of MD simulations without additional salt. CKPM refers to the version with Berger/Chiu NH_3 charges compatible with Berger (i.e. the NH_3 group having the same charges as in the $N(CH_3)_3$ group of the PC lipids; 'M' stands for Mukhopadhyay after the first published Berger-based PS simulation that used these charges) and CKP refers to the version with more Gromos compatible version (i.e. the charges for the NH_3 group taken from the lysine side-chain).

lipid/counter-ions	force field for lipids / ions	NaCl (mM)	$CaCl_2$ (mM)	[a]N_l	[b]N_w 4.	[c]N_c	[d]T (K)	[e]t_{sim}(ns)	[f]t_{anal} (ns)	[g]files
DOPS/Na^+	CHARMM36 [**?**] 5.	0	0	128	4480	0	303	500	100	[22]
DOPS/Na^+	CHARMM36ua [**?**] 6.	0	0	128	4480	0	303	500	100	[23]
DOPS/Na^+	Slipids [24]	0	0	128	4480	0	303	500	100	[25]
DOPS/Na^+	Slipids [24]	0	0	288	11232	0	303	200	100	[26]
DOPS/Na^+	Berger [27]	0	0	128	4480	0	303	500	100	[28]
DOPS/Na^+	GROMOS-CKP1 [**?**] 7.	0	0	128	4480	0	303	500	100	[29]
DOPS/Na^+	GROMOS-CKP2 [**?**] 8.	0	0	128	4480	0	303	500	100	[30]
DOPS/Na^+	lipid17 [31] / JC [32]	0	0	128	4480	0	303	600	100	[33]
DOPS/Na^+	lipid17 [31] / ff99 [34]	0	0	128	4480	0	303	600	100	[35]
POPS/Na^+	CHARMM36 [**?**] 9.	0	0	128	4480	0	298	500	100	[36]
POPS/K^+	CHARMM36 [**?**] 10.	0	0	128	4480	0	298	500	100	[37]
POPS/Na^+	CHARMM36ua [**?**] 11.	0	0	128	4480	0	298	500	100	[38]
POPS/Na^+	Slipids [24]	0	0	128	4480	0	298	500	100	[39]
POPS/Na^+	Berger [**?**]	0	0	128	4480	0	298	500	100	[40]
POPS/Na^+	MacRog [41]	0	0	?	??	0	?	?	?	[**?**] 12.
OPPS/Na^+	MacRog [41]	0	0	128	5120	0	298	200	100	[42]
POPS/Na^+	GROMOS-CKPM [**?**] 13.	0	0	128	4480	0	298	500	100	[43]
POPS/Na^+	GROMOS-CKP [**?**] 14.	0	0	128	4480	0	298	500	100	[44]
POPS/Na^+	lipid17 [31] / JC [32]	0	0	128	4480	0	298	600	100	[45]
POPS/Na^+	lipid17 [31] / ff99 [34]	0	0	128	4480	0	298	600	100	[46]

[a]Number of lipid molecules with largest mole fraction
[b]Number of water molecules
[c]Number of additional cations
[d]Simulation temperature
[e]Total simulation time
[f]Time used for analysis
[g]Reference for simulation files

RESULTS AND DISCUSSION

Headgroup and glycerol backbone order parameters measured from POPS lipid bilayer

Figure 1 summarizes the experimental NMR results for POPS bilayer sample. showing one single splitting for beta (which gives an order parameter equal to 0.12), and for alpha a superposition of a large splitting (order parameter equal to 0.09) and a very small splitting which cannot resolved with the available resolution. S-DROSS slice for beta clearly shows that the order parameter is negative, which is confirmed by SIMPSON simulations using the The S-DROSS slice for alpha suggests that the higher order parameter is positive and the deviation towards negative values in the longer t1 times suggests that the smaller order parameter is negative. This is confirmed by SIMPSON simulation using value of 0.09 for the larger alpha order parameter and the value of -0.02 for smaller (black curve). The value for the smaller alpha order parameter for SIMPSON calculation was taken from Fig 3 in Ref. 52, because resolution in 13C NMR experiments was nor high enough to determine numerical value for this. The S-DROSS curve from SIMPSON simulation with positive value for the smaller order parameter (dashed grey), did not agree with experiments confirming the interpretation that the smaller order parameter is negative.

The headgroup and glycerol backbone order parameters of POPS measured in this work are compared to the literature values of DOPS [53] and POPC [19] in Fig. 2. Our results for POPS are in good agreement with the previously reported values for DOPS measured with ^{2}H NMR. Significant differences are observed between PC and PS lipids, especially at the headgroup region. Previous discussions in the literature have concluded that glycerol backbone structure is largely similar in PC, PE, PG and PS lipids [17]. The headgroup region was found to be similar in PC, PE and PG lipid (assuming that the signs of PE and PG order parameters are the same as in PC), while the PS headgroup was suggested to be more rigid [54, 55]. The detailed structural differences between the headgroups is, however, not known.

TABLE II: List of MD simulations. The salt concentrations calculated as [salt]=$N_c \times$[water] / N_w, where [water] = 55.5 M. CKPM refers to the version with Berger/Chiu NH_3 charges compatible with Berger (i.e. the NH_3 group having the same charges as in the $N(CH_3)_3$ group of the PC lipids; 'M' stands for Mukhopadhyay after the first published Berger-based PS simulation that used these charges [**?**]) and CKP refers to the version with more Gromos compatible version (i.e. the charges for the NH_3 group taken from the lysine side-chain).

lipid/counter-ions	force field for lipids / ions	NaCl (mM)	$CaCl_2$ (mM)	[a]N_l	[b]N_w 15.	[c]N_c	[d]T (K)	[e]t_{sim}(ns)	[f]
POPC:POPS (5:1)/K^+	CHARMM36 [47**?**] 16.	0	0	110:22	4935	0	298	100	
POPC:POPS (5:1)/K^+	CHARMM36 [**?**]	0	0	250:50	?	0	298	200	
POPC:POPS (5:1)/K^+	CHARMM36 [**?**]	0	0	110:22	4620	0	298	500	
POPC:POPS (5:1)/Na^+	CHARMM36 [**?**]	0	0	110:22	4620	0	298	500	
POPC:POPS (1:1)/K^+	CHARMM36 [**?**]	0	0	150:150	?	0	298	200	
POPC:POPS (5:1)	CHARMM36 [**?**]20.	0	150 21.	250:50	?	?	298	200	
POPC:POPS (5:1)	CHARMM36 [**?**]23.	0	1000 24.	250:50	?	?	298	200	
POPC:POPS26. (5:1)/K^+	MacRog [41]	0	0	120:24	5760	0	298	200	
POPC:POPS (5:1)/K^+	MacRog [41]	0	100	120:24	5760	10	298	200	
POPC:POPS (5:1)/K^+	MacRog [41]	0	300	120:24	5760	31	298	200	
POPC:POPS (5:1)/K^+	MacRog [41]	0	1000	120:24	5760	104	298	200	
POPC:POPS (5:1)/K^+	MacRog [41]	0	3000	120:24	5760	311	298	200	

32.MacRog simulations with KCl to be added

33.Berger simulations with NaCl and CaCl to be added

[a]Number of lipid molecules with largest mole fraction
[b]Number of water molecules
[c]Number of additional cations
[d]Simulation temperature
[e]Total simulation time
[f]Time used for analysis
[g]Reference for simulation files

Headgroup and glycerol backbone in simulations of PS lipid bilayers without additional ions

The headgroup order parameters of DOPS and POPS bilayers from different simulation models are compared with the experimental data in Fig. 3. In line with the previous study for PC lipids [9], the glycerol backbone order parameters in CHARMM36 roughly agree with the experimental data, while significant discrepancies for glycerol backbone carbons are observed in other models. **38.Discussion is to be finished.**

39.Also the discussion about POPS/OPPS issue with MacRog model should be added.

Based on the subjective ranking shown in Fig. 4, the CHARMM36 is the best performing model for both lipids. However, none of the tested models give a satisfactory agreement with experiments for the headgroup order paramaters of PS lipids. The total deviation from the experiments (Σ in Fig. 4) for the best performing CHARMM36 model is larger for PS lipids (8) than for PC (3) [9]. Therefore the interpretation of structural details of PS headgroup or differences between PC and PS lipids is very challenging from the current MD simulation models. Figures 16 and 17 show dihedral angle distributions calculated from different models. The glycerol backbone structures from CHARMM36 and Slipids simulations visualized in Fig. 5 reveal the missing structures in Slipids model, which probably lead to the incorrect order parameters. For the headgroup α and β carbon order parameters of PS lipids, the tested models perform less well than for PC headgroup in previous study [9]. **40.Discussion is to be finished. One possible conclusion could be the following: The main differences between the models in the headgroup region are observed for dihedrals C12-C11-O12-P and C11-C12-C13-O1A. CHARMM36, CHARMM36UA and Slipids give very similar results to the dihedral C11-C12-C13-O1A, which is close to the β-carbon. The order parameters of β-carbons for these three models are in best argeement with the experiments in figure 3. On the other hand, Gromos-CKP models give better order parameters for α-carbon than Slipids, CHARMM36 or CHARMM36UA. In conclusion, the suggestion would be that the single peak for observed at 120 degrees in CHARMMs and Slipids would be more realistic for C11-C12-C13-O1A dihedral, while the single peak at 180 degrees observed in CKP models and in Berger would be most realistic for C12-C11-O12-P dihedral.**

Counterion binding to lipid bilayers containing PS lipids

Since systems with negatively charged PS lipids always contain counterions and the ion binding presumably affects the PS headgroup order parameters, the discussion of ion binding affinity and headgroup structure cannot be separated as done previously for PC lipids [9, 10]. The density profiles of counterions along membrane normal from different simulations show significant binding of counterions in bilayers in all models in Fig. 6. Differences are, however, observed in the total binding affinity and in the shape of density profiles. Comparison of bulk concentrations suggests that strongest bind-

FIG. 1: (a) The headgroup region of the INEPT spectrum with headgroup and glycerol backbone carbons assigned. (b) 2D R-PDLF spectra for headgroup and glycerol backbone regions. (c) Slices for α and β barbons. (d) Experimental SDROSS data (points) and SIMPSON simulations (lines). Order parameter values of -0.12 for the β-carbon, and 0.09 and -0.02 for the larger and smaller α-carbon slittings were used in the SIMPSON calculations. The S-DROSS curve from SIMPSON simulation with positive value for the smaller order parameter (dashed grey).

34.This is preliminary figure, should be polished. 35.Should we show slices for all the analyzed carbons in (c)?

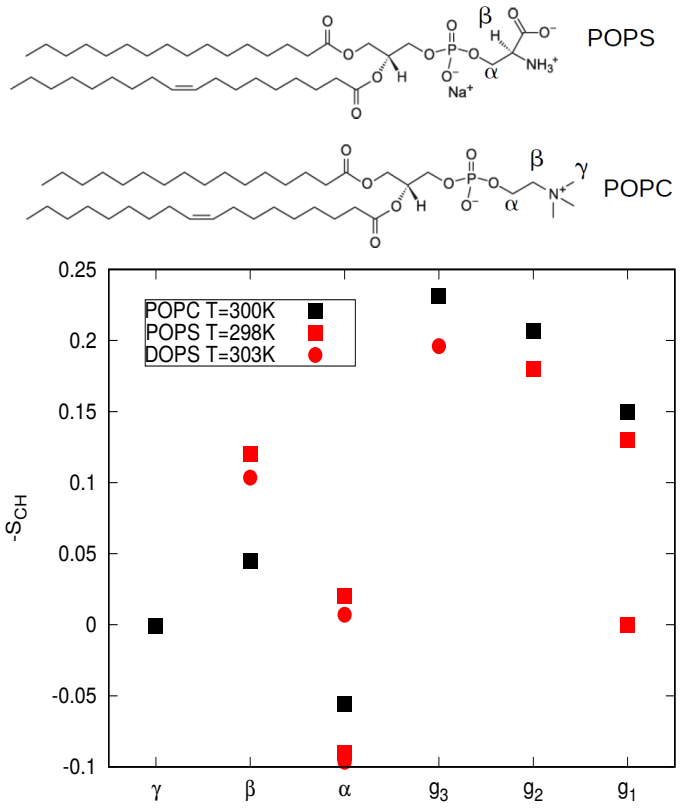

FIG. 2: Headgroup and glycerol backbone order parameters of POPS measured in this work compared with values for DOPS (^{2}H NMR, 0.1M of NaCl) [53] and POPC (^{13}C NMR) [19] from literature. Signs for PS order parameters as measured in this work and signs for PC as measured in Refs [16**?**].

ing is observed in MacRog, Berger and Lipid17 models, respectively. Other models gives roughly similar total binding affinity based on rough comparison of bulk concentrations. In CHARMM36, CHARMM36ua and Gromos-CKP models two maxima are observed in sodium density plots, possible corresponding binding to phoshate and carboxylic grops in the PS headgroup. In other models only a single maxima is observed.

41.More quantitative analysis of binding positions and affinity may be useful.

Based on previous simulation results it has been suggested that the counterion binding and concomitant screening of headgroup repulsion leads to smaller area per lipid in PS lipid bilayers than in PC bilayers [27, 56, 57]. Therefore we also show the area per lipid from different models in Fig. 6. The proposed trend is observed for Lipid17 model, for which the Joung-Cheatham ions give higher affinity and smaller area per molecule. However, the trend is not observed when comparing accross different force fields. For example, CHARMM36ua and MacRog give similar area per molecule but binding affinity is significantly higher in MacRog. On the other hand, Gromos-CKP models gives a larger area per lipid than other models, being only in agreement with experiments [58], but the binding affinity is comparable to the CHARMM36, CHARMM36us and Slipids, which give smaller are per molecule.

In order to compare the sodium interaction with PS containing membranes between experiments and simulations, Fig. 7 shows the headgroup order parameters of POPC and POPS measured from 5:1 mixture as a function of different monovalent ions added to the buffer. The experimental experimental results [59] are compared with different simulation models. In line with the trend observed for bilayers in the absence of negatively charged lipids [**?**], the POPC headgroup order parameter response to lithium ions is significantly larger than to potassium, indicating stronger binding of lithium ions to lipid bilayers. The unique nature of lithium is also evident in the response of PS headgroup order parameters to bounds ions, which decrease with the addition of lithium or divalent cations but increase with the addition of sodium or potassium. The headgroup order parameter response to the added NaCl in the Berger model is similar to the experiments of LiCl, except for the α carbon of POPS for which the change is overestimated with the order of magnitude. The results suggests that the binding affinity of sodium is overestimated by the Berger model, in line with the previous results [10], and that the response of α carbon of POPS to the added sodium is significantly overestimated. The response of POPC to the added potassium in MacRog model is only slightly overestimated, in

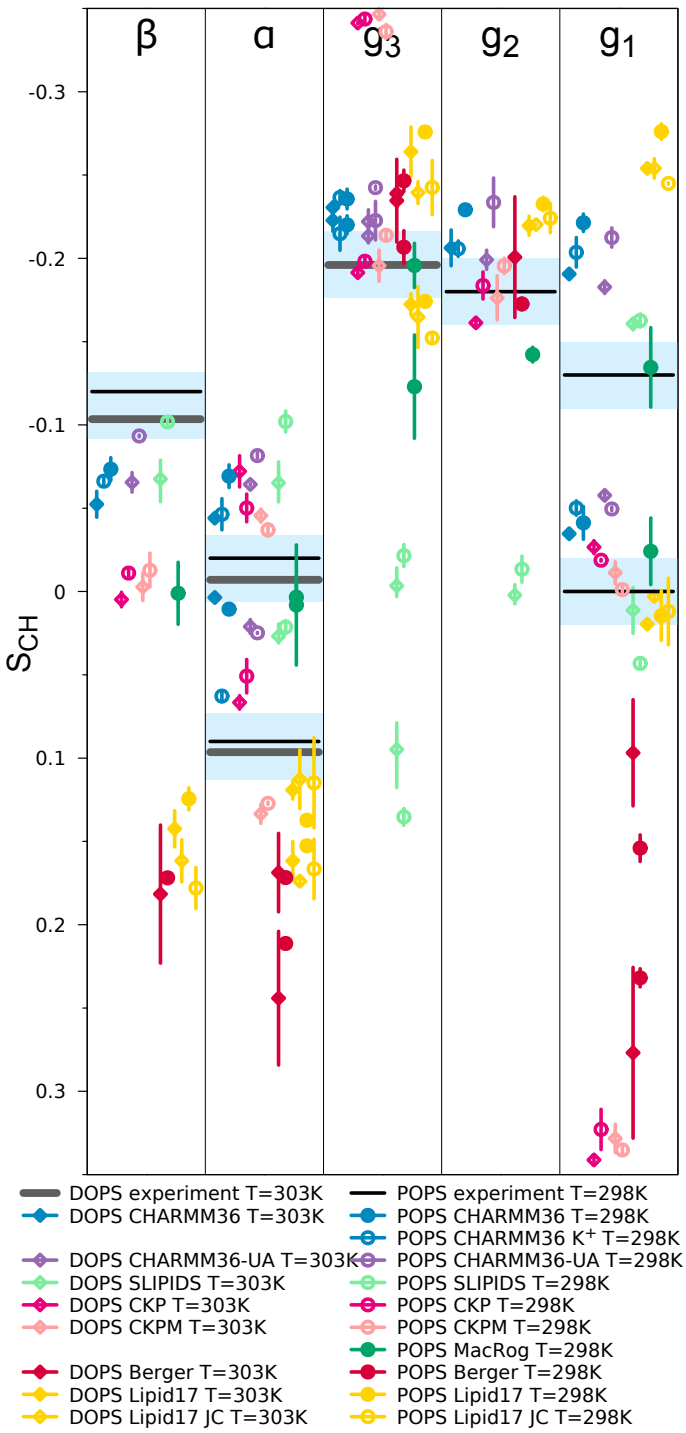

FIG. 3: Order parameters for PS headgroup and glycerol backbone from simulations with different models and experiments without $CaCl_2$. All DOPS data at 303 K, POPS at 298 K. Experimental data from [53] contain 0.1 M of NaCl. Signs are taken from experiments for POPS described in Supplementary Information. The vertical bars shown are not error bars, but demonstrate that we had at least two data sets; the ends of the bars mark the extreme values from the sets, and the dot marks their measurement-time-weighted average.

	β	α	g_3	g_2	g_1	Σ
CHARMM 36	M	M F	M	M	**M F**	8
CHARMM 36-UA	M	M	M	M	**M** F	8
GROMOS-CKP1	**M**	M **F**	**M F**		**M F**	14
GROMOS-CKP2	**M**	M F	**M F**		**M F**	14
Slipid	M	**M**	**M F**	**M**	M **F**	14
Berger	**M**	**M F**	M F	M	**M F**	15

FIG. 4: Rough subjective ranking of force fields based on Figure 3. Here M indicates a magnitude problem, F a forking problem; letter size increases with problem severity. Color scheme: within experimental error (dark green), almost within experimental error (light green), clear deviation from experiments (light red), and major deviation from experiments (dark red). The Σ-column shows the total deviation of the force field, when individual carbons are given weights of 0 (matches experiment), 1, 2, and 4 (major deviation). For full details of the assessment, see Supplementary Information.

36.Issue about possible updates to this plot:

https://github.com/NMRLipids/NMRlipidsIVotherHGs/issues/4

37.Lipid17 and MacRog results should be added into this plot.

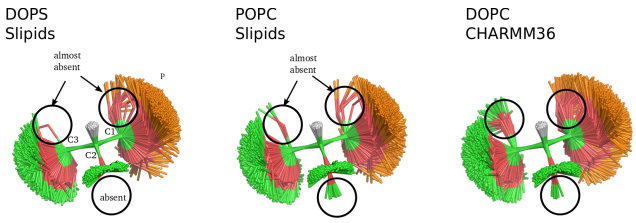

FIG. 5: Snapshots overlayed from different simulations for glycerol backbone region by Pavel Buslaev.

contrast to the response of POPS where order of magnitude overestimations of reposonse are observed. In conclusion, it seems that the response of PS headgroup to bound cations is not correctly captured in the tested models. **44.Finish the discussion when more models are available**

Headgroup structure in PS and PC mixtures

Cellular membranes often compose of mixtures of zwitterionic and negatively charged lipids. The response of PC headgroup to mixtures of differently charged lipids are collected

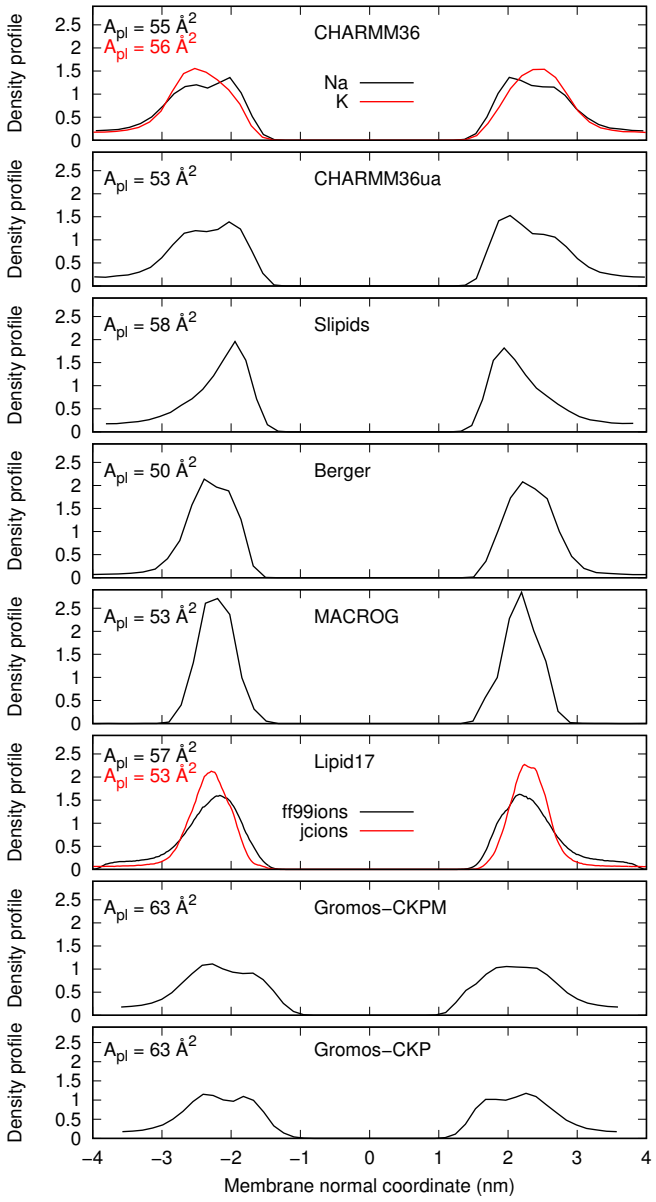

FIG. 6: Counterion densities of POPS lipid bilayer along the membrane normal from simulations with different force fields.

from different experiments in Fig. 12. As expected from the electrometer concept [60], the headgroup order parameters increase with the addition of negatively charged PS and PG lipids, decrease when mixed with positively charged surfactants and are less affected by the addition of zwitterionic PE lipids or cholesterol. In addition to the results summarized in Fig. 12, also mixtures of PC with negatively charged PI, CL, PA, and zwitterionic SM follow the eletrometer concept [18].

Fig. 9 shows the PC and PS headgroup order parameters from POPC:POPS mixtures with various mole fractions from simulations and experiments [7, 18]. The experimentally observed increase of PC headgroup order parameters with the increasing amount of negatively charged PS lipid is reproduced in MacRog simulations with potassium counterions, but not in CHARMM36 simulations with potassium or sodium conterions. The results can be understood from the counterion density distributions shown in Fig. 8. Both counterions are more strongly bound to bilayers in CHARMM36 simulations than potassium in MacRog simulation. The cation binding probably neutralizes the effect of negatively charged lipids in CHARMM36 simulations, while the weaker binding of potassium in MacRog simulations enables the increase of order parameters with the added amount of PS. **46.This discussion will be finalized when we have the results for monovalent ions also from other simulations.**

Also the headgroup order parameters of POPS mixed with varying amounts of POPC from simulations and experiments [7, 61] are shown in Fig. 9. The β-carbon order parameter of POPS slightly decreases and positive order parameter of α-carbon slightly increases with increasing amount of PS lipids. This may indicate increasing order of the headgroup. **49.The existing literature about this should be mentioned/discussed.** It should be, however, noted that the experimental data for pure POPS and POPC/POPS mixture come from different experimental sets, 13C NMR in this work and 2H NMR from Ref. 7, respectively. Therefore the accuracy of the order parameter change is not as high as typically in the measurements of order parameter changes, see discussion about qualitative and quantitative accuracy in Ref. 11. The changes of PS headgroup order parameters are not reproduced by the tested simulation models. The β-carbon order parameter increase with increasing amount of PS in CHARMM36 and MacRog simulations in contrast to the experimental data. The smaller α-carbon order parameter increase in both simulation models with increasing amount of PS, while it is almost unchanged in experiments. The larger α-carbon order parameter increase in MacRog and decrease in CHARMM36 with increasing amount of PS, both model exhibiting a poor agreement with experiments. Signifincant improvement in the MD simulation models are needed to interpret the PS headgroup structures and mutual interactions with PC lipids. **50.This discussion should be updated.**

Ca^{2+} binding affinity in bilayers with negatively charged PS lipids

The headgroup order parameters of PC lipids decrease proportionally to the bound positive charge in to a bilayer [10, 60] and can be therefore used to measure the ion binding affinity. This molecular electrometer concept can be also applied to lipid bilayers with mixtures of PC and negatively charged lipids [7, 61, 62] (see Fig. 13).

The headgroup order parameter changes of POPC and POPS from POPC:POPS (5:1) mixtures are shown in Fig. 10 as a function of Ca^{2+} concentration from different simulations and experiments [7]. The ion density distributions from the simulations are shown in Fig. 11. The results suggest that

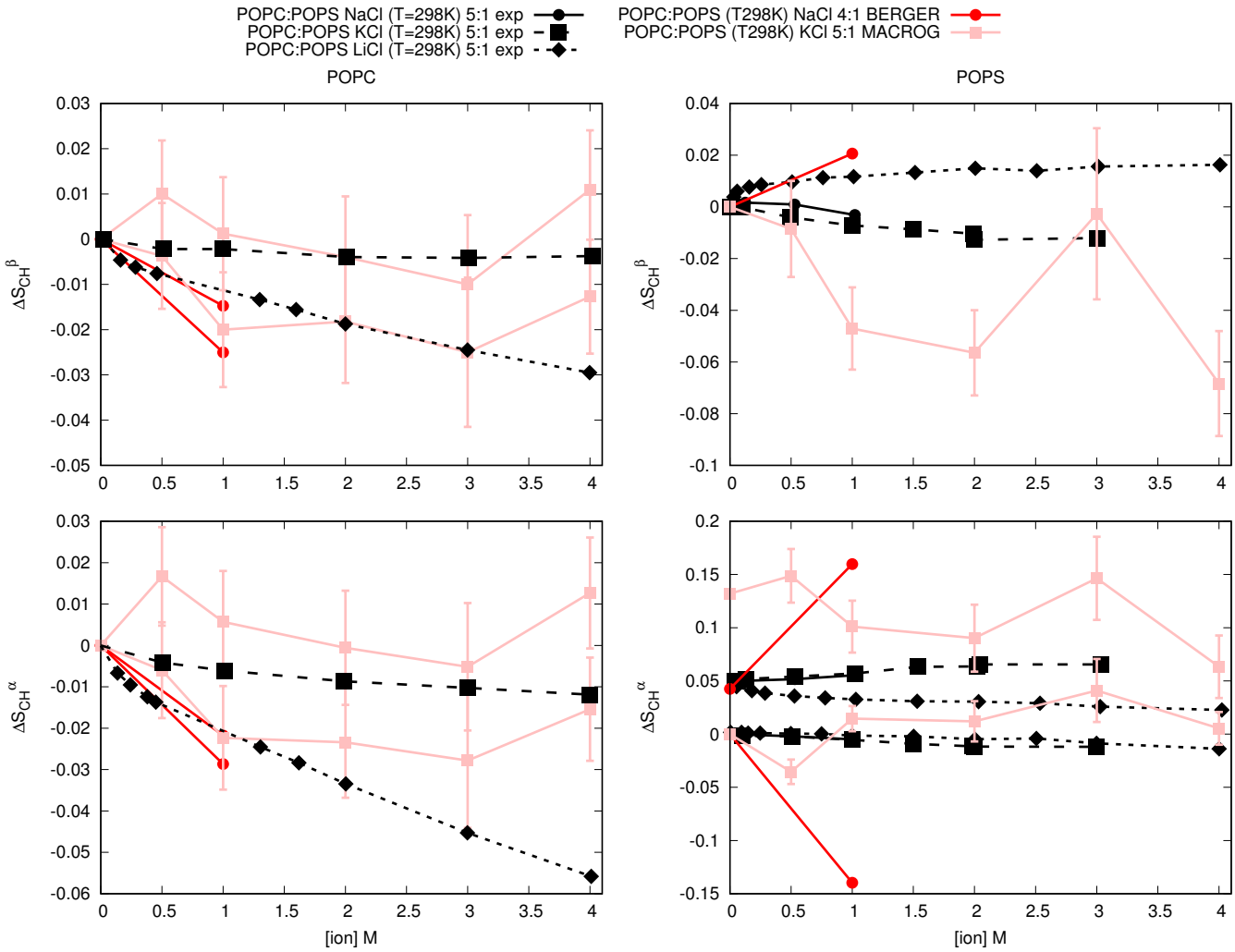

FIG. 7: Changes of the PC (left) and PS (right) headgroup order parameters as a function of added NaCl, KCl and LiCl from POPC:POPS (5:1) mixture. The experimental data is from Ref. 7. The values from counterion-only systems are set as a zero point of y-axis. To correctly illustrate the significant forking of the α-carbon order parameter in PS headgroup (bottom, right), the y-axis is tranferred with the same value for both order parameters such that the lower order parameter value is at zero.

42.The upcoming results from Lipid17 have been mentioned in the blog:

http://nmrlipids.blogspot.com/2017/12/nmrlipids-iv-current-status-and.html?showComment=1522151331118#c5876812436739342658

43.Maybe we should get the CHARMM results as well?

Ca^{2+} ions clearly overbind in simulations with MacRog and Berger models, as expected from previous results for PC lipid bilayers [10]. It should be noted, however, that the lowest concentration (100mM) gives a good agreemet with experiments **51.Should be analyze/discuss this further? Binding with ∼100 mM is saturated in both Berger and MacRog simulations. Maybe this is realistic? It should be noted that Berger simulation do not have counterions.**. Surprisingly, the calcium binding seems to be too weak CHARMM36 simulations. This is due to the NBfix interaction parameters from Ref. 63, incorporated in the parameters from CHARMM-GUI at the time of running the simulations (January 2018). The binding of calcium to pure POPC bilayer is also too weak with these parameters as shown in Figs. 19 and 20. **52.The discussion is to be finished when we have all the data in the plot.**

Also the order parameters of PS headgroup from POPC:POPS (5:1) mixture are shown in Fig. 10 as a function of $CaCl_2$ concentration. In experiments the order parameters exhibit a strong dependence of $CaCl_2$ with small concentrations with a rapid saturation around 50 mM. The changes of PS headgroup order parameters with added $CaCl_2$ are overestimated in all tested simulation models. Furthermore, the changes of the headgroup order parameters do not qualitatively agree with experiments. This is in contrast to previous results for PC headgroup [10], where qualitatively correct reponse to bound ions was observed despite of significant discrepancies in the headgroup structure without additional ions.

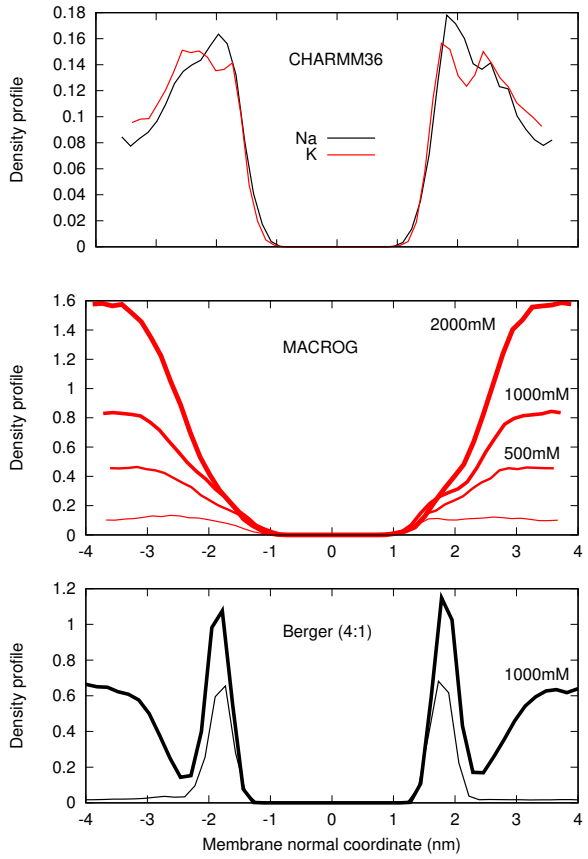

FIG. 8: Counterion density distributions from PC:PS mixtures.

45.Fix CKP1 and CKP2 captions.

CONCLUSIONS

SUPPLEMENTARY INFORMATION

Simulated systems

CHARMM36

59.To be written by Piggot, Madsen and Ollila

CHARMM36ua

60.To be written by Piggot

Slipids

61.To be written by Piggot and Favela

Berger

62.To be wiritten by Piggot and Ollila Simulations with sodium were taken directly from Ref. **?** and simulations with calcium directly from 8. Simulation of POPC at 310 K was taken directly from Ref. 64.

GROMOS-CKP

63.To be written by Piggot

Lipid17

64.To be written by Kav and Miettinen

MacRog

65.To be written by Javanainen and Piggot

PC lipid headgroup response to different mixtures in experiments

As shown in Fig. 12, order parameters of PC headgroup behave in various lipid mixtures as expected from the electrometer concept [18, 60], i.e., order parameters increase when anionic lipids are mixed with PC and decrease with cationic surfactants. The changes with the addition of neutral lipids is significantly smaller.

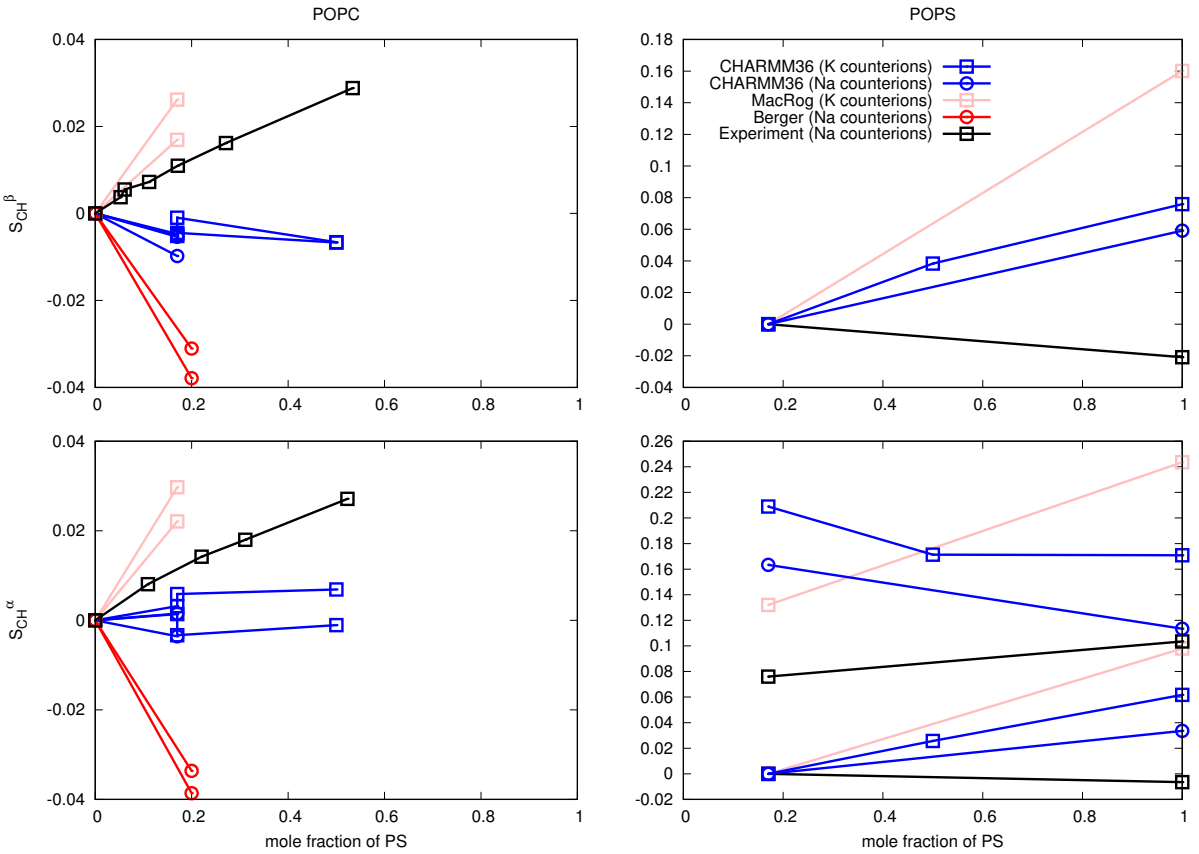

FIG. 9: Changes of PC (left panel) and PS (right panel) headgroup order parameters from POPC:POPS mixtures with increasing amount of POPS. Experimental results of POPC are taken from Ref. 18 (signs are determined as discussed in [9, 11]). Experimental values for POPS in pure bilayer and in mixture are measured in this work and in Ref. 7 at 298K, respectively. For POPC (left panel) the zero point of y-axis is set to the value of pure bilayer. For β-carbon of POPS (right panel, top) the zero point of y-axis is set to the value from POPC:POPS (5:1) mixture. For α-carbon of POPS (right panel, bottom) the y-axis is tranferred with the same value for both order parameters such that the lower order parameter value from POPC:POPS (5:1) mixture is at zero to correctly illustrate the significant forking.

47.Simulation of CHARMM36 at 298K should be maybe rerun with Gromacs 5.

48.The upcoming results from Lipid17 have been mentioned in the blog:

http://nmrlipids.blogspot.com/2017/12/nmrlipids-iv-current-status-and.html?showComment=1522151331118#c5876812436739342658

Cation binding affinity to lipid bilayers with different amount of charge

Before using the headgroup order parameters to compare ion binding affinity between simulations and experiments, it is important to quantify the response of the order parameters to the bound charge in simulations. The response of headgroup order parameters to the fixed amount of cationic surfactants in POPC bilayer is compared between simulations and experiments [65] In Fig. 15. The figure shows that the order parameters are too sensitive to bound charge in Lipid14 model, while CHARMM36 is in better agreement with experiments. This has to be taken into account when analysin the binding affinities.

Difference between POPC and OPPS in MacRog model

Dihedrals

Dihedrals

The experimental results show essentially no changes in the order parameters as a function of added NaCl, while significant changes are observed in simulations. However, the minimum buffer concentration of NaCl in the experimental was 100mM [59]. Therefore, we cannot exclude the possibility that the NaCl induced changes were already saturated with 100mM NaCl concentration, which was the case for $CaCl_2$ in Fig. 10.

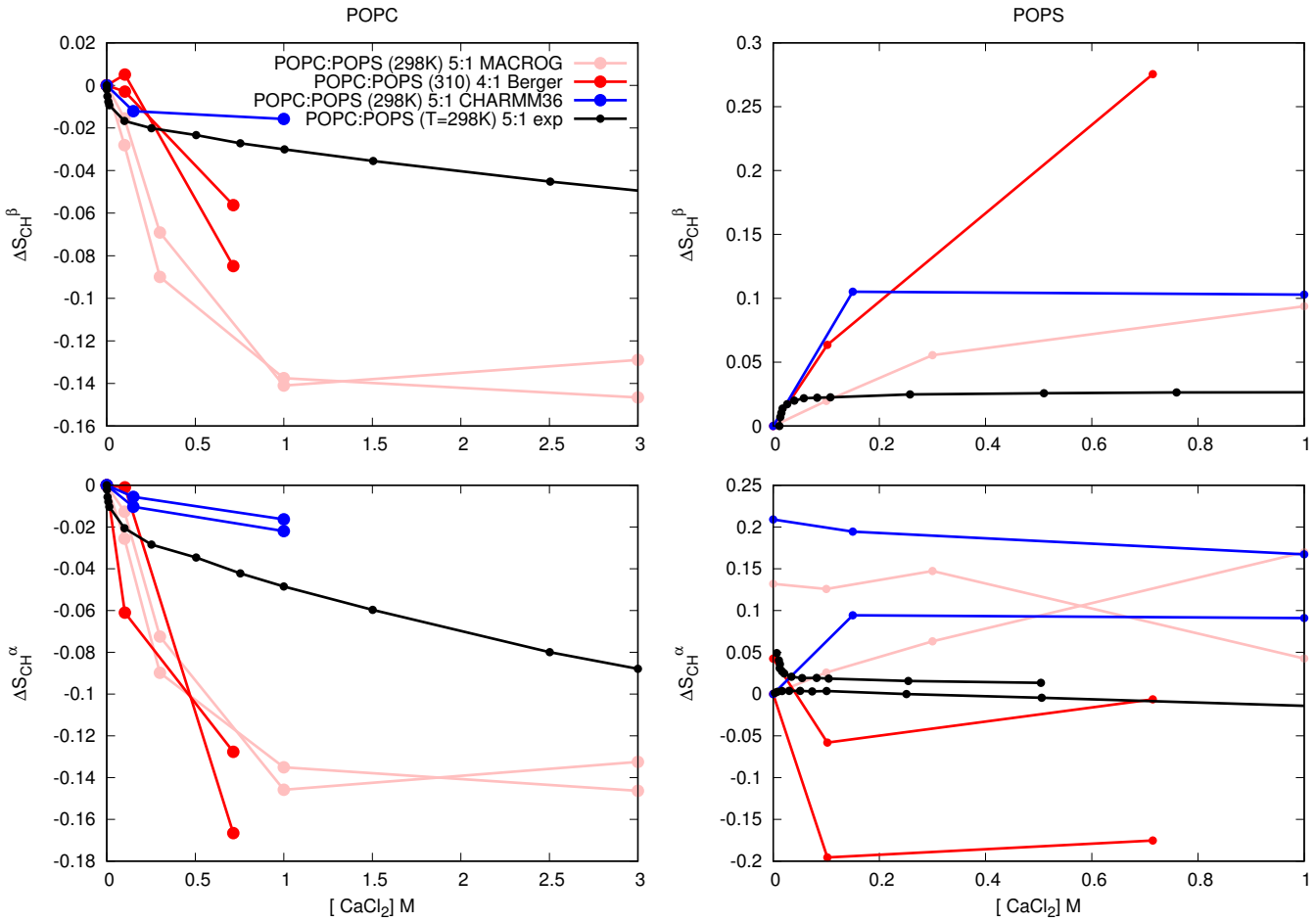

FIG. 10: Changes of POPC (left) and POPS (right) headgroup order parameters in POPC:POPS (5:1) mixture as a function $CaCl_2$ concentration. Experimental data is taken from 7. The values from counterion-only systems are set as a zero point of y-axis. To correctly illustrate the significant forking of the α-carbon order parameter in PS headgroup (bottom, right), the y-axis is tranferred with the same value for both order parameters such that the lower order parameter value is at zero.

53.Information about the cuonterions in different simulations should be added

54.Upcoming simulations with original CHARMM36 have been mentioned in the blog:
http://nmrlipids.blogspot.com/2017/12/nmrlipids-iv-current-status-and.html?showComment=1520090718976#c5569269391707740056

55.Upcoming Lipid17 simulations have been mentioned in the blog
http://nmrlipids.blogspot.com/2017/12/nmrlipids-iv-current-status-and.html?showComment=1515177306419#c994825612316235467

Details of the rough subjective force field ranking (Fig. 4)

The assessment was based fully on the Fig. 3. First, for each carbon (the columns in Fig. 3) in each force field (the rows), we looked separately at deviations in magnitude and forking.

Magnitude deviations, i.e., how close to the experimentally obtained C–H order parameters (OPs) the force-field-produced OPs were. For each carbon, the following 5-step scale was used:

0 ( ): More than half of all the calculated OPs (that is, of all different hydrogens in all different lipids) were within the *subjective sweet spots* (SSP, blue-shaded areas in Fig. 3).

1 (M): All the calculated OPs were < 0.03 units away from the SSP.

2 (M): All the calculated OPs were < 0.05 units away from the SSP.

3 (M): All the calculated OPs were < 0.10 units away from the SSP.

4 (M): Some of the calculated OPs were > 0.10 units away from the SSP.

Forking deviations, i.e., how well the difference in order parameters of two hydrogens attached to a given carbon matched that obtained experimentally. Note that this is not relevant for β and g_2, which have only one hydrogen. For the

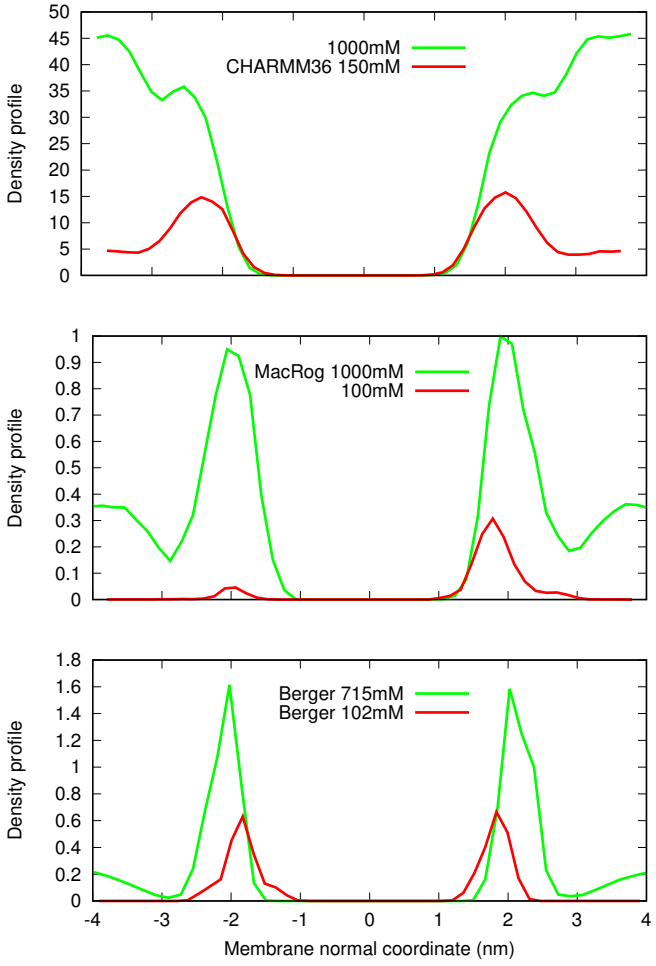

FIG. 11: Ca2+ density profiles from simulations.

56.The CHARMM results are mass densities, numbers should be used.

57.Should we include also counterions into the plot?

58.Not all the data from MacRog is included.

α carbon, for which a considerable forking of 0.105 is experimentally seen, the following 5-step scale was used:

0 ( ): The distance D between the dots (that mark the measurement-time-weighted averages in Fig. 3) was $0.08 < D < 0.13$ units for all the calculated OPs (that is, for all different lipids).

1 (F): $(0.06 < D < 0.08)$ OR $(0.13 < D < 0.15)$.

2 (F): $(0.04 < D < 0.06)$ OR $(0.15 < D < 0.17)$.

3 (F): $(0.02 < D < 0.04)$ OR $(0.17 < D < 0.19)$.

4 (F): $(D < 0.02)$ OR $(0.19 < D)$.

For the g_3 carbon, for which no forking is indicated by experiments, the following 5-step scale was used:

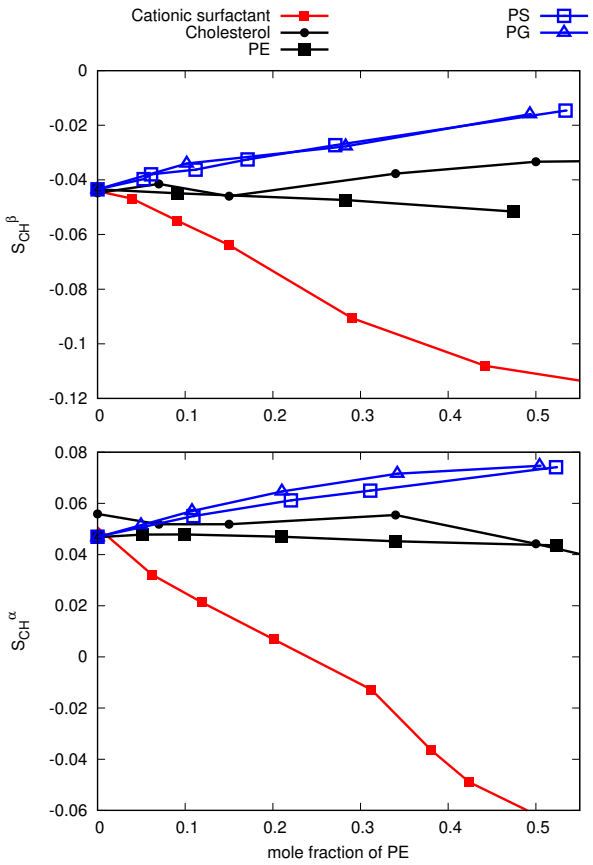

FIG. 12: PC headgroup order parameters from experiments of mixtures with PE, PS, PG and cholesterol [18, 19, 65]. Signs are determined as discussed in [9, 11].

0 ( ): $D < 0.02$.

1 (F): $0.02 < D < 0.04$.

2 (F): $0.04 < D < 0.06$.

3 (F): $0.06 < D < 0.08$.

4 (F): $0.08 < D$.

For the g_1 carbon, for which a considerable forking of 0.13 is experimentally seen, the following 5-step scale was used:

0 ( ): $0.11 < D < 0.15$.

1 (F): $(0.09 < D < 0.11)$ OR $(0.15 < D < 0.17)$.

2 (F): $(0.07 < D < 0.09)$ OR $(0.17 < D < 0.19)$.

3 (F): $(0.05 < D < 0.07)$ OR $(0.19 < D < 0.21)$.

4 (F): $(D < 0.05)$ OR $(0.21 < D)$.

Based on these assessments of magnitude and forking deviations, each carbon was then assigned to one of the following groups: ”within experimental error” (magnitude and forking deviations both on step 0 of the scales described above), ”almost within experimental error” (sum of the magnitude and

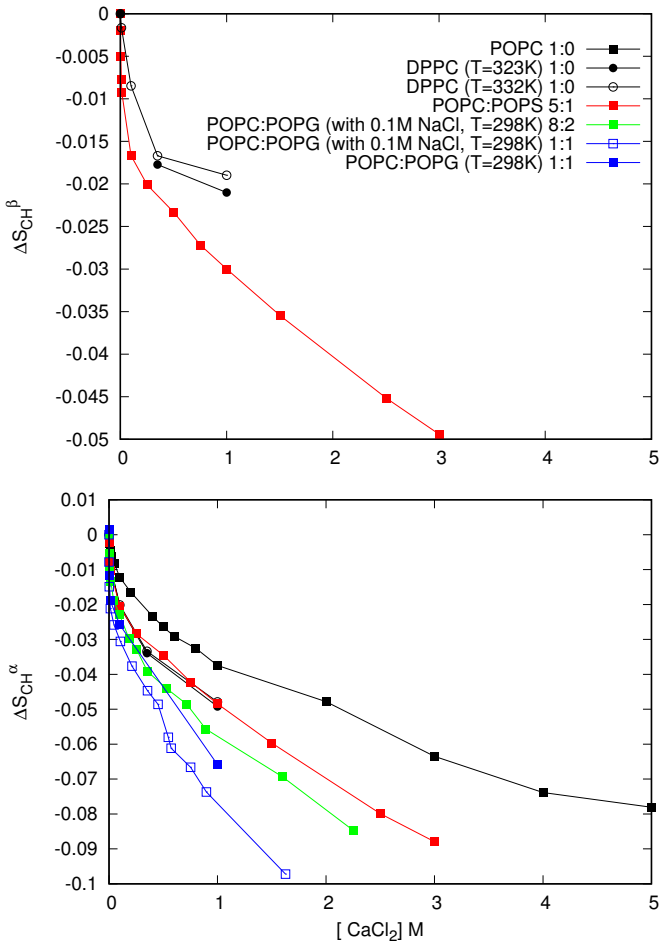

FIG. 13: The change of PC headgroup order parameters as a function of $CaCl_2$ measured from bilayers containing different amount of negatively charged lipids. The values are taken from 2H NMR experiments reported in the literature (DPPC [66], POPC [67], POPC:POPS (5:1) [7], POPC:POPG mixtures with 0.1M NaCl [62] and POPC:POPG (1:1) without NaCl [61]). As expected, the decrease of order parameters with the added $CaCl_2$ is more pronounced for systems with larger fraction of negatively charged lipids, indicating larger amount amount of bound cations.

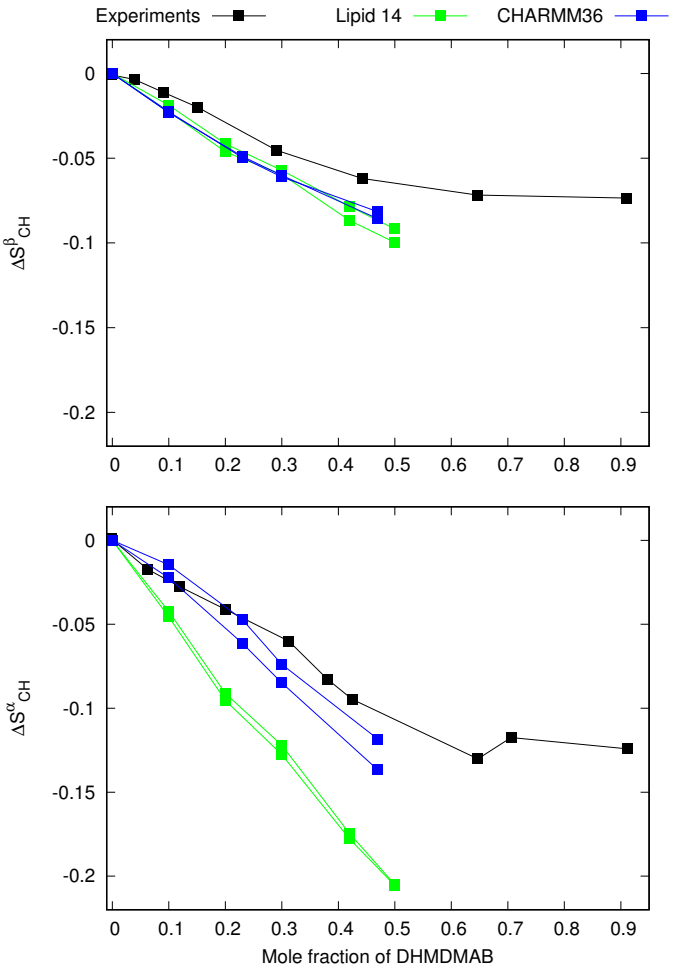

FIG. 14: The response of headgroup order parameters to the fixed amount of cationic surfactants in POPC bilayer is compared between simulations and experiments [65].

forking deviation steps 1 or 2), "clear deviation from experiments" (sum of magnitude and forking deviation steps from 3 to 5), and "major deviation from experiments" (sum of magnitude and forking deviation steps from 6 to 8). These groups are indicated by colors in Fig. 4. (Note that for β and g_2, for which there can be no forking, the corresponding group assigment limits were: 0, 1, 2, and 3.)

Finally, the total ability of the force field to describe the headgroup and glycerol structure was estimated. To this end, the groups were given the following weights: 0 (within experimental error), 1 (almost within experimental error), 2 (clear deviation from experiments), 4 (major deviation from experiments), and the weights of the five carbons were summed up. The sum, given in the Σ-column of Fig. 3, was then used to

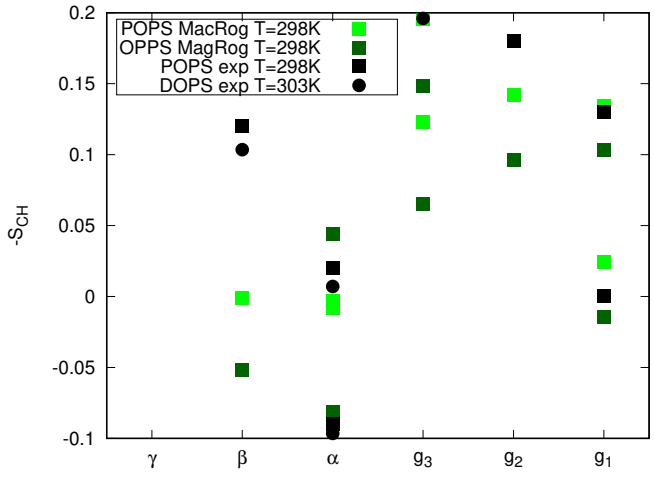

FIG. 15: Headgroup order parameters from POPS and OPPS simulations with MacRog model.

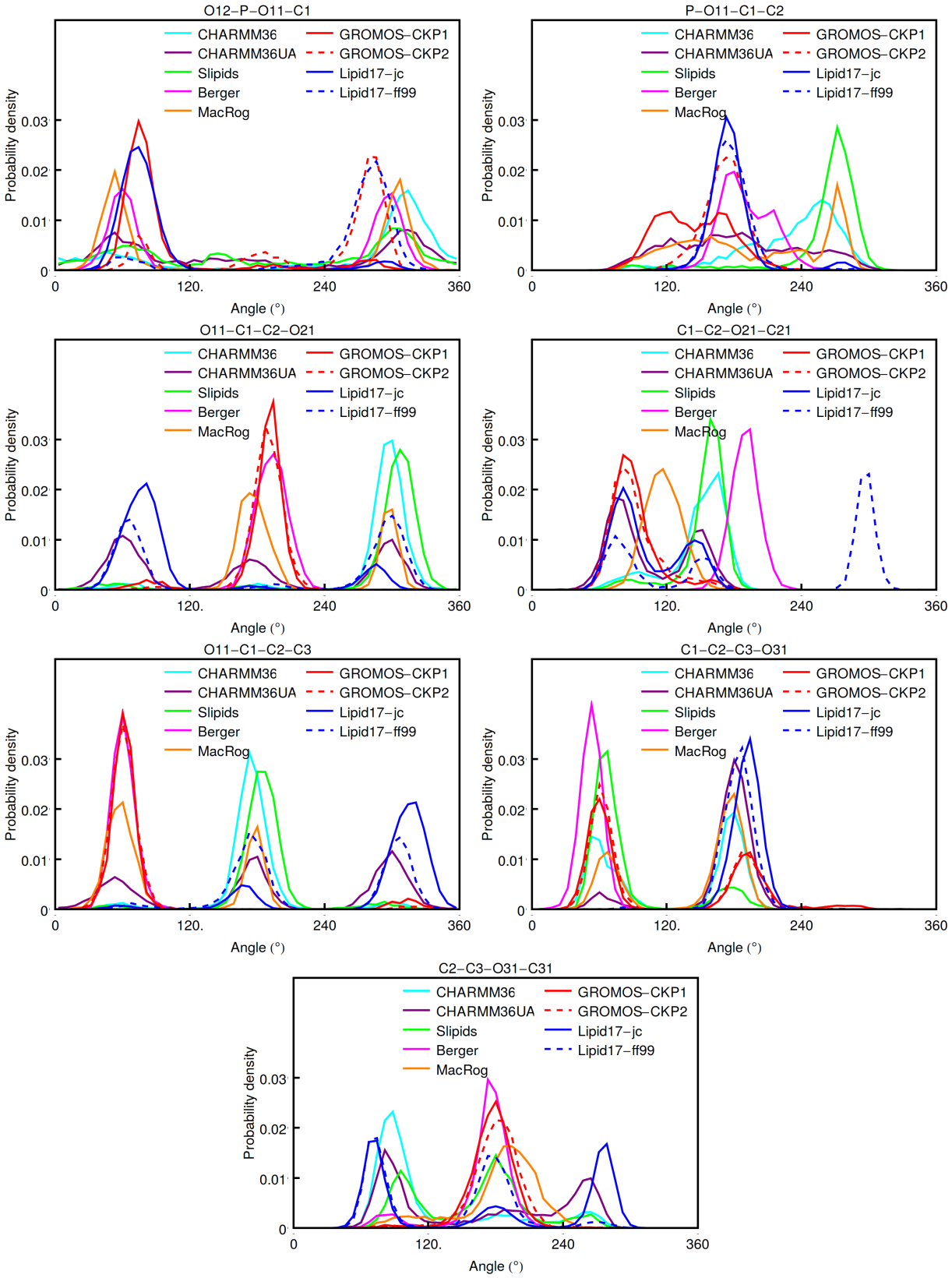

FIG. 16: Dihedral angle distributions of bonds from phosphate to acyl chain carbonyls from different simulation models.

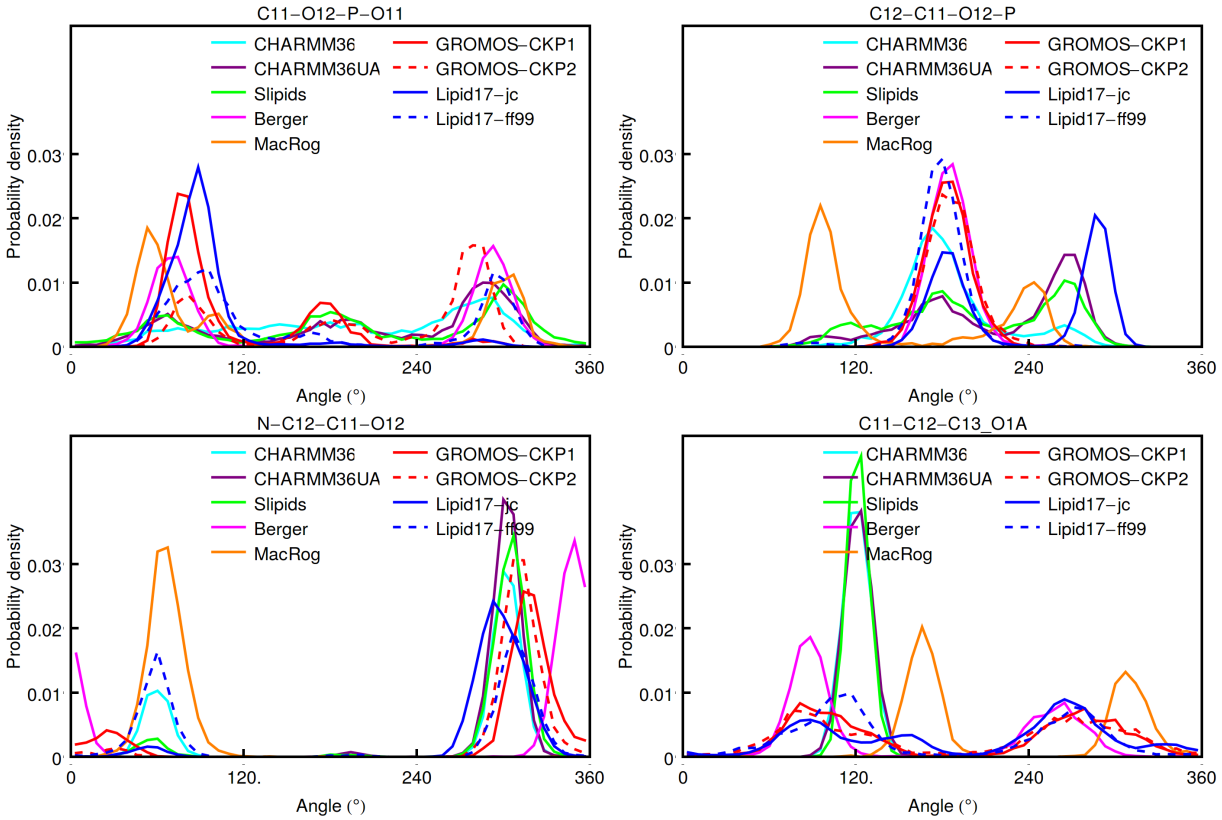

FIG. 17: Dihedral angle distributions of bonds from phosphate to headgroup from different simulation models.

(roughly and subjectively, as should be clear from the above description) rank the force fields.

* samuli.ollila@helsinki.fi

[1] M. A. Lemmon, Nat. Rev. Mol. Cell Biol. **9**, 99 (2008).

[2] P. A. Leventis and S. Grinstein, Annual Review of Biophysics **39**, 407 (2010).

[3] L. Li, X. Shi, X. Guo, H. Li, and C. Xu, Trends in Biochemical Sciences **39**, 130 (2014), ISSN 0968-0004.

[4] T. Yeung, G. E. Gilbert, J. Shi, J. Silvius, A. Kapus, and S. Grinstein, Science **319**, 210 (2008).

[5] H. Zhao, E. K. J. Tuominen, and P. K. J. Kinnunen, Biochemistry **43**, 10302 (2004).

[6] G. P. Gorbenko and P. K. Kinnunen, Chemistry and Physics of Lipids **141**, 72 (2006).

[7] M. Roux and M. Bloom, Biochemistry **29**, 7077 (1990).

[8] A. Melcrová, S. Pokorna, S. Pullanchery, M. Kohagen, P. Jurkiewicz, M. Hof, P. Jungwirth, P. S. Cremer, and L. Cwiklik, Sci. Reports **6**, 38035 (2016).

[9] A. Botan, F. Favela-Rosales, P. F. J. Fuchs, M. Javanainen, M. Kanduč, W. Kulig, A. Lamberg, C. Loison, A. Lyubartsev, M. S. Miettinen, et al., J. Phys. Chem. B **119**, 15075 (2015).

[10] A. Catte, M. Girych, M. Javanainen, C. Loison, J. Melcr, M. S. Miettinen, L. Monticelli, J. Maatta, V. S. Oganesyan, O. H. S. Ollila, et al., Phys. Chem. Chem. Phys. **18**, 32560 (2016).

[11] O. S. Ollila and G. Pabst, Biochimica et Biophysica Acta (BBA) - Biomembranes **1858**, 2512 (2016).

[12] J. Seelig, Cell Biology International Reports **14**, 353 (1990), ISSN 0309-1651, URL http://www.sciencedirect.com/science/article/pii/030916519091204H.

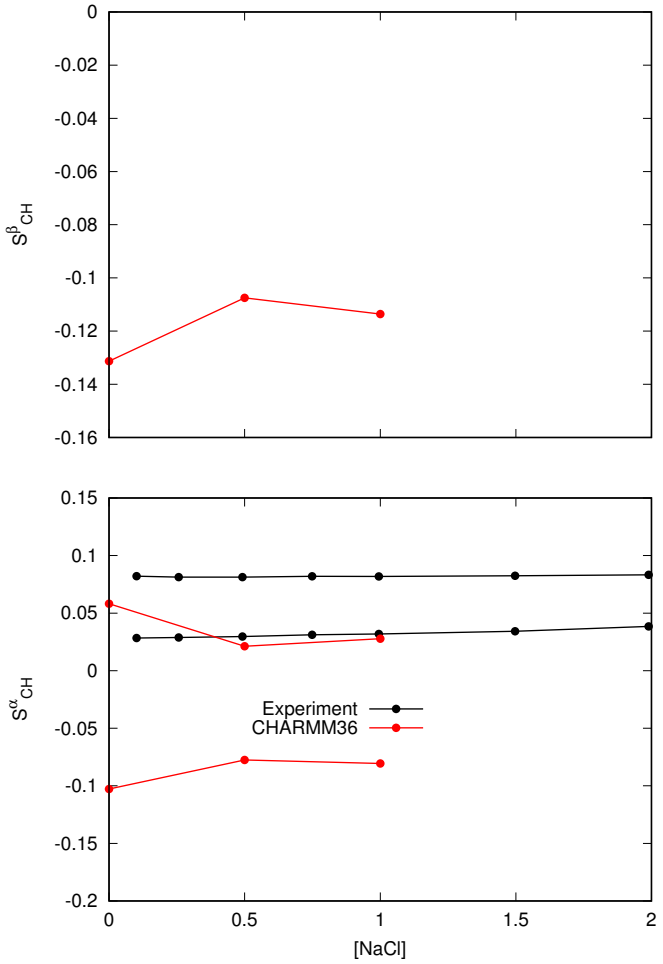

FIG. 18: Order parameters of PS headgroup as a function of added NaCl measured from DMPC:DMPS (3:1) mixture [59].

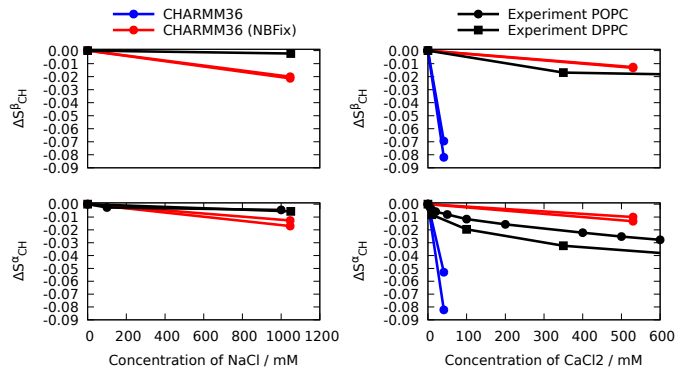

FIG. 19: The response of headgroup order parameters to the fixed amount of cationic surfactants in POPC bilayer is compared between simulations and experiments [65].

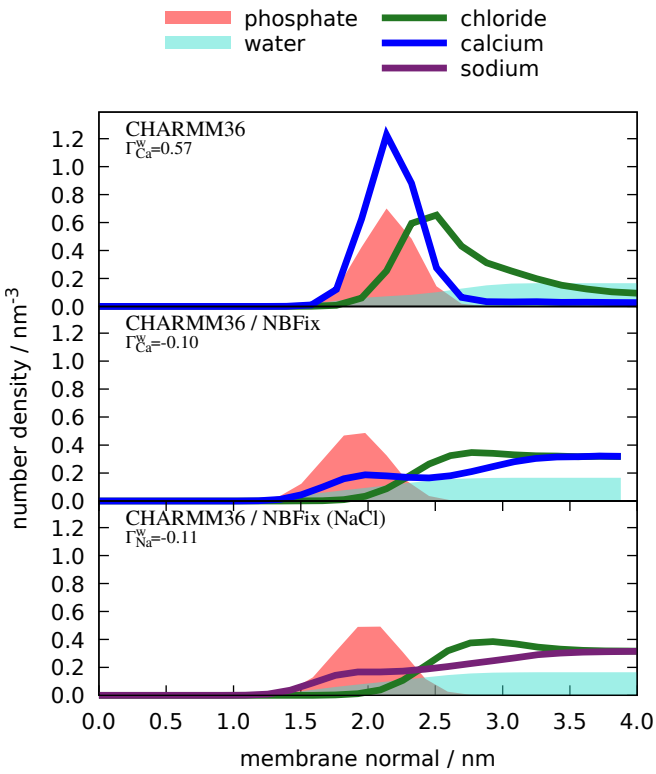

FIG. 20: The response of headgroup order parameters to the fixed amount of cationic surfactants in POPC bilayer is compared between simulations and experiments [65].

[13] C. G. Sinn, M. Antonietti, and R. Dimova, Colloids and Surfaces A: Physicochemical and Engineering Aspects **282-283**, 410 (2006), a Collection of Papers in Honor of Professor Ivan B. Ivanov (Laboratory of Chemical Physics and Engineering, University of Sofia) Celebrating his Contributions to Colloid and Surface Science on the Occasion of his 70th Birthday.

[14] P. T. Vernier, M. J. Ziegler, and R. Dimova, Langmuir **25**, 1020 (2009).

[15] J. M. Boettcher, R. L. Davis-Harrison, M. C. Clay, A. J. Nieuwkoop, Y. Z. Ohkubo, E. Tajkhorshid, J. H. Morrissey, and C. M. Rienstra, Biochemistry **50**, 2264 (2011).

[16] T. M. Ferreira, R. Sood, R. Bärenwald, G. Carlström, D. Topgaard, K. Saalwächter, P. K. J. Kinnunen, and O. H. S. Ollila, Langmuir **32**, 6524 (2016).

[17] H. U. Gally, G. Pluschke, P. Overath, and J. Seelig, Biochemistry **20**, 1826 (1981).

[18] P. Scherer and J. Seelig, EMBO J. **6** (1987).

[19] T. M. Ferreira, F. Coreta-Gomes, O. H. S. Ollila, M. J. Moreno, W. L. C. Vaz, and D. Topgaard, Phys. Chem. Chem. Phys. **15**, 1976 (2013).

[20] S. V. Dvinskikh, H. Zimmermann, A. Maliniak, and D. Sandstrom, J. Magn. Reson. **168**, 194 (2004).

[21] J. D. Gross, D. E. Warschawski, and R. G. Griffin, J. Am. Chem. Soc. **119**, 796 (1997).

[22] T. Piggot, *CHARMM36 DOPS simulations (versions 1 and 2) 303 K 1.0 nm LJ switching* (2017), URL `https://doi.org/10.5281/zenodo.1129411`.

[23] T. Piggot, *CHARMM36-UA DOPS simulations (versions 1 and 2) 303 K 1.0 nm LJ switching* (2017), URL `https://doi.`

org/10.5281/zenodo.1129456.
[24] J. P. M. Jämbeck and A. P. Lyubartsev, Phys. Chem. Chem. Phys. **15**, 4677 (2013).
[25] T. Piggot, *Slipids DOPS simulations (versions 1 and 2) 303 K 1.0 nm cut-off with LJ-PME* (2017), URL https://doi.org/10.5281/zenodo.1129439.
[26] F. Favela-Rosales, *MD simulation trajectory of a fully hydrated DOPS bilayer: SLIPIDS, Gromacs 5.0.4. 2017.* (2017), URL https://doi.org/10.5281/zenodo.495510.
[27] P. Mukhopadhyay, L. Monticelli, and D. P. Tieleman, Biophysical Journal **86**, 1601 (2004).
[28] T. Piggot, *Berger DOPS simulations (versions 1 and 2) 303 K 1.0 nm cut-off* (2017), URL https://doi.org/10.5281/zenodo.1129419.
[29] T. Piggot, *GROMOS-CKP DOPS simulations (versions 1 and 2) 303 K with Berger/Chiu NH3 charges and PME* (2017), URL https://doi.org/10.5281/zenodo.1129429.
[30] T. Piggot, *GROMOS-CKP DOPS simulations (versions 1 and 2) 303 K with GROMOS NH3 charges and PME* (2017), URL https://doi.org/10.5281/zenodo.1129447.
[31] I. Gould, A. Skjevik, C. Dickson, B. Madej, and R. Walker, *Lipid17: A comprehensive amber force field for the simulation of zwitterionic and anionic lipids* (2018), in preparation.
[32] I. S. Joung and T. E. Cheatham, The Journal of Physical Chemistry B **112**, 9020 (2008).
[33] B. Kav and M. S. Miettinen, *Molecular dynamics simulation trajectory of an anionic lipid bilayer: 100 mol% DOPS with Na+ counterions using Joung-Cheetham Ions* (2018), B.K acknowledges financial support from International Max Planck Research School on Multiscale Bio-Systems, URL https://doi.org/10.5281/zenodo.1134871.
[34] J. Åqvist, J. Phys. Chem. **94**, 8021 (1990).
[35] B. Kav and M. S. Miettinen, *Molecular dynamics simulation trajectory of an anionic lipid bilayer: 100 mol% DOPS with Na+ counterions using ff99 Ions* (2018), B.K acknowledges financial support from International Max Planck Research School on Multiscale Bio-Systems, URL https://doi.org/10.5281/zenodo.1135142.
[36] T. Piggot, *CHARMM36 POPS simulations (versions 1 and 2) 298 K 1.0 nm LJ switching* (2017), URL https://doi.org/10.5281/zenodo.1129415.
[37] T. Piggot, *CHARMM36 POPS simulations (versions 1 and 2) 298 K 1.0 nm LJ switching with K ions* (2018), URL https://doi.org/10.5281/zenodo.1182654.
[38] T. Piggot, *CHARMM36-UA POPS simulations (versions 1 and 2) 298 K 1.0 nm LJ switching* (2017), URL https://doi.org/10.5281/zenodo.1129458.
[39] T. Piggot, *Slipids POPS simulations (versions 1 and 2) 298 K 1.0 nm cut-off with LJ-PME* (2017), URL https://doi.org/10.5281/zenodo.1129441.
[40] T. Piggot, *Berger POPS simulations (versions 1 and 2) 298 K 1.0 nm cut-off* (2017), URL https://doi.org/10.5281/zenodo.1129425.
[41] A. Maciejewski, M. Pasenkiewicz-Gierula, O. Cramariuc, I. Vattulainen, and T. Róg, J. Phys. Chem. B **118**, 4571 (2014).
[42] M. Javanainen, *Simulation of a pops bilayer* (2017), URL https://doi.org/10.5281/zenodo.1120287.
[43] T. Piggot, *GROMOS-CKP POPS simulations (versions 1 and 2) 298 K with Berger/Chiu NH3 charges and PME* (2017), URL https://doi.org/10.5281/zenodo.1129431.
[44] T. Piggot, *GROMOS-CKP POPS simulations (versions 1 and 2) 298 K with GROMOS NH3 charges and PME* (2017), URL https://doi.org/10.5281/zenodo.1129435.
[45] M. S. Miettinen and B. Kav, *Molecular dynamics simulation trajectory of an anionic lipid bilayer: 100 mol% POPS with Na+ counterions using Joung-Cheatham Ions* (2018), B.K. acknowledges financial support from International Max Planck Research School on Multiscale Bio-Systems., URL https://doi.org/10.5281/zenodo.1148495.
[46] M. S. Miettinen and B. Kav, *Molecular dynamics simulation trajectory of an anionic lipid bilayer: 100 mol% POPS with Na+ counterions using ff99 ions* (2018), B.K. acknowledges financial support from International Max Planck Research School on Multiscale Bio-Systems, URL https://doi.org/10.5281/zenodo.1134869.
[47] J. B. Klauda, R. M. Venable, J. A. Freites, J. W. O'Connor, D. J. Tobias, C. Mondragon-Ramirez, I. Vorobyov, A. D. MacKerell Jr, and R. W. Pastor, J. Phys. Chem. B **114**, 7830 (2010).
[48] O. H. S. Ollila, *POPS+83%popc lipid bilayer simulation at T298K ran CHARMM_GUI force field and Gromacs* (2017), URL https://doi.org/10.5281/zenodo.1011104.
[49] T. Piggot, *CHARMM36 POPS/POPC simulations (versions 1 and 2) 298 K 1.0 nm LJ switching with K ions* (2018), URL https://doi.org/10.5281/zenodo.1182658.
[50] T. Piggot, *CHARMM36 POPS/POPC simulations (versions 1 and 2) 298 K 1.0 nm LJ switching with Na ions* (2018), URL https://doi.org/10.5281/zenodo.1182665.
[51] M. Javanainen, *Simulations of popc/pops membranes with cacl_2.* (2017), URL https://doi.org/10.5281/zenodo.897467.
[52] M. Roux and M. Bloom, Biophys. J. **60**, 38 (1991).
[53] J. L. Browning and J. Seelig, Biochemistry **19**, 1262 (1980).
[54] R. Wohlgemuth, N. Waespe-Sarcevic, and J. Seelig, Biochemistry **19**, 3315 (1980).
[55] G. Büldt and R. Wohlgemuth, The Journal of Membrane Biology **58**, 81 (1981), ISSN 1432-1424, URL http://dx.doi.org/10.1007/BF01870972.
[56] S. A. Pandit and M. L. Berkowitz, Biophysical Journal **82**, 1818 (2002).
[57] U. R. Pedersen, C. Leidy, P. Westh, and G. H. Peters, Biochimica et Biophysica Acta (BBA) - Biomembranes **1758**, 573 (2006).
[58] J. Pan, X. Cheng, L. Monticelli, F. A. Heberle, N. Kucerka, D. P. Tieleman, and J. Katsaras, Soft Matter **10**, 3716 (2014).
[59] M. Roux and J.-M. Neumann, FEBS Letters **199**, 33 (1986).
[60] J. Seelig, P. M. MacDonald, and P. G. Scherer, Biochemistry **26**, 7535 (1987).
[61] F. Borle and J. Seelig, Chemistry and Physics of Lipids **36**, 263 (1985).
[62] P. M. Macdonald and J. Seelig, Biochemistry **26**, 1231 (1987).
[63] S. Kim, D. Patel, S. Park, J. Slusky, J. Klauda, G. Widmalm, and W. Im, Biophysical Journal **111**, 1750 (2016), ISSN 0006-3495, URL http://www.sciencedirect.com/science/article/pii/S0006349516307615.
[64] S. Ollila, M. T. Hyvönen, and I. Vattulainen, J. Phys. Chem. B **111**, 3139 (2007).
[65] P. G. Scherer and J. Seelig, Biochemistry **28**, 7720 (1989).
[66] H. Akutsu and J. Seelig, Biochemistry **20**, 7366 (1981).
[67] C. Altenbach and J. Seelig, Biochemistry **23**, 3913 (1984).

ToDo

P.

1. Authorship query to be sent soon. 1